THE JOURNAL OF BIOLOGICAL CHEMISTRY VOL. 282, NO. 20, pp. 15258–15270, May 18, 2007

Regulation of the Rab5 GTPase-activating Protein RN-tre by the Dual Specificity Phosphatase Cdc14A in Human Cells*

Received for publication, January 31, 2007, and in revised form, March 16, 2007 Published, JBC Papers in Press, March 19, 2007, DOI 10.1074/jbc.M700914200

Letizia Lanzetti[‡1], Valentina Margaria[‡1,2], Fredrik Melander[§], Laura Virgili[‡], Myung-Hee Lee[§], Jiri Bartek[§], and Sanne Jensen[§3]

From the [‡]Dipartimento di Scienze Oncologiche, Università degli Studi di Torino, Istituto per la Ricerca e la Cura del Cancro, Strada Provinciale 142, 10060 Candiolo, Torino, Italy and the [§]Institute of Cancer Biology and Centre for Genotoxic Stress Research, Danish Cancer Society, Strandboulevarden 49, DK-2100 Copenhagen, Denmark

The Cdc14 family of dual specificity phosphatases regulates key mitotic events in the eukaryotic cell cycle. Although extensively characterized in yeast, little is known about the function of mammalian Cdc14 family members. Here we report a genetic substrate-trapping system designed to identify substrates of the human Cdc14A (hCdc14A) phosphatase. Using this approach, we identify RN-tre, a GTPase-activating protein for the Rab5 GTPase, as a novel physiological target of hCdc14A. As a Rab5 GTPase-activating protein, RN-tre has previously been implicated in control of intracellular membrane trafficking. We find that RN-tre forms a stable complex with the catalytically inactive hCdc14A C278S mutant but not with the wild type protein in human cells, indicative of a substrate/enzyme interaction. In support, we show that RN-tre is regulated by cell cycle-dependent phosphorylation peaking at mitosis, which can be antagonized by hCdc14A activity *in vitro* as well as *in vivo*. Furthermore, we show that RN-tre phosphorylation is critical for efficient hCdc14A association and that RN-tre binding can be displaced by tungstate, a competitive inhibitor that binds to the active site of hCdc14A. Consistent with the preference of hCdc14A for phosphorylations mediated by proline-directed kinases, we find that RN-tre is a direct substrate of cyclin-dependent kinase. Finally, phosphorylation of RN-tre appears to finely modulate its catalytic activity. Our findings reveal a novel connection between the cell cycle machinery and the endocytic pathway.

In eukaryotes, accurate cell cycle progression and survival rely on the evolutionarily conserved dual specificity phosphatase Cdc14, a member of the protein-tyrosine phosphatase family (1, 2). The founding member in budding yeast belongs to a group of proteins called the mitotic exit network (MEN),[4] which inactivates mitotic cyclin-dependent kinase (Cdk) activity and is required for mitotic exit and cytokinesis (3). A central upstream component of the MEN is the GTPase Tem1, which belongs to the Rab subfamily of small GTPases (4). Activation of Tem1 triggers a signaling cascade at the spindle pole bodies, the equivalent of the mammalian centrosome, implicating multiple protein kinases, which ultimately lead to Cdc14 activation (5–7).

The activity of yeast Cdc14 is mainly regulated at the level of its subcellular localization. Through much of the cell cycle, Cdc14 is sequestered in the nucleolus and kept inactive through association with Net1 as part of the RENT complex (8, 9). Early in anaphase, a pool of Cdc14 is released from the nucleolus through Cdk-dependent phosphorylation of Net1 mediated by the FEAR (fourteen early anaphase release) regulatory network (10, 11). This initial wave of Cdc14 release activates in a positive feedback loop the MEN, which is necessary for the complete and sustained nucleolar release of Cdc14 (12). Once released, Cdc14 promotes mitotic Cdk inactivation by dephosphorylating the anaphase-promoting complex specificity factor Cdh1, thereby stimulating destruction of mitotic cyclins (13). In addition, Cdc14 dephosphorylates the Cdk inhibitor Sic1 and its transcription factor Swi5, which leads to accumulation of stable Sic1, whereby mitotic Cdk is further inactivated (14).

Unrelated to its function in Cdk inactivation, Cdc14 plays an important role in microtubule dynamics during anaphase (15). Dephosphorylation of the kinetochore component Ask1 appears to be critical for anaphase microtubule stability (15). Also, Cdc14 has been shown to dephosphorylate the Sli15/INCENP subunit of the aurora B kinase complex, thereby targeting the complex to the anaphase spindle (16), suggesting that Cdc14 may have multiple targets and functions at the mitotic spindle in budding yeast.

Despite their structural similarities, the function of Cdc14 phosphatases appears to differ across species. In *Schizosaccharomyces pombe*, the Cdc14 homolog, Clp1/Flp1, is not required for mitotic exit but rather is essential for regulating septum

* This work was supported by the Danish National Research Foundation and the Danish Cancer Society (to J. B.); the Danish Cancer Society and Novo Nordisk Foundation (to S. J.); Svenska Sällskapet för Medicinsk Forskning, Stockholm (to F. M.); and Associazione Italiana per la Ricerca sul Cancro, the European Community (VI Framework), and Association for International Cancer Research (AICR) (to L. L.). The costs of publication of this article were defrayed in part by the payment of page charges. This article must therefore be hereby marked "*advertisement*" in accordance with 18 U.S.C. Section 1734 solely to indicate this fact.

[1] These authors contributed equally to this work.

[2] Supported by a fellowship from AICR.

[3] To whom correspondence should be addressed: Evolva A/S, Bülowsuej 25, DK-1870 Frederiksberg, Denmark. Tel.: 4532502028; Fax: 4535283885; E-mail: sannej@evolva.com.

[4] The abbreviations used are: MEN, mitotic exit network; X-gal, 5-bromo-4-chloro-3-indolyl-β-D-galactopyranoside; Cdk, cyclin-dependent kinase; siRNA, small interfering RNA; MAPK, mitogen-activated protein kinase; GAP, GTPase-activating protein; PBS, phosphate-buffered saline; HA, hemagglutinin; WT, wild type; PD, phosphatase-dead; GST, glutathione *S*-transferase; GFP, green fluorescent protein; DTT, dithiothreitol; LSB, Laemmli sample buffer.

formation and cytokinesis as a member of the septation initiation network (17), a signaling pathway homologous to the MEN. Clp1/Flp1 also regulates entry into mitosis by antagonizing mitotic Cdk activity during G_2 (18, 19). Unlike budding yeast Cdc14, Clp1/Flp1 does not dephosphorylate the Rum1 and Ste9 proteins, homologues of Sic1 and Cdh1, respectively, but instead inhibits mitotic Cdk activity by promoting the inhibitory phosphorylation of Cdk on Tyr^{15} through activation of Wee1 and inhibition of Cdc25 (19, 20). Similar to its budding yeast ortholog, Clp1/Flp1 localizes predominantly to the nucleolus during G_1 and S phases but is released from this confinement during prophase to translocate to the mitotic spindle, the spindle pole bodies, and the medial ring (18, 20).

In *Caenorhabditis elegans*, the Cdc14 homolog localizes to the central spindle and the midbody, and depletion of Ce-CDC-14 has been reported to cause defects in cytokinesis (21). However, interestingly, Ce-CDC-14 was shown to be required for the quiescent state of specific precursor cells. In this study, it was proposed that Ce-CDC-14 contributes to a G_1 cell cycle arrest by promoting accumulation of the Cdk inhibitor, CKI-1 (22), reminiscent of the scenario in budding yeast, where Cdc14 regulates the abundance of Sic1.

In humans, there are two Cdc14 homologues, hCdc14A and hCdc14B, whose functions in cell cycle progression are poorly understood. The two isoforms share 50% sequence identity but have different C-terminal domains. Human Cdc14A localizes dynamically to interphase but not mitotic centrosomes and appears to regulate the function of this organelle *in vivo* (23, 24). Depletion of hCdc14A by siRNA leads to a delay in centrosome separation and cytokinetic defects (23). During mitosis, hCdc14A concentrates at the spindle midzone and the midbody (24, 25), suggesting a direct involvement in cytokinesis. Much less is known about the function of hCdc14B, which localizes to interphase nucleoli and to the spindle apparatus during mitosis (23, 24, 26). Human Cdc14B displays microtubule bundling and stabilizing activities and may play a role in modulating spindle dynamics during mitosis (27). The dramatic differences in their localization profiles suggest that hCdc14A and hCdc14B perform different tasks in the cell.

Cdc14 from diverse species share a conserved core of ~350 amino acids located toward the N terminus, which harbors the conserved protein-tyrosine phosphatase signature motif $HCX_5R(S/T)$. The protein-tyrosine phosphatases are a diverse family of enzymes that comprises tyrosine-specific, dual specificity Cdc25 and low molecular weight phosphatases (28). *In vitro* studies have shown that hCdc14A has the preference for substrates of proline-directed kinases, such as Cdks and mitogen-activated protein kinases (MAPKs), modified at pS/pT-P motifs, similar to its yeast counterpart (14, 24). This specificity is further corroborated by the crystal structure of the core domain of human Cdc14B (29). In particular, hCdc14A was shown to dephosphorylate hCdh1 and reconstitute active hCdh1/anaphase-promoting complex *in vitro* (30), suggesting that Cdc14A has the potential also to trigger mitotic Cdk inactivation in human cells. In addition, hCdc14 is capable of dephosphorylating the INCENP protein *in vitro* (25), implying that it may regulate the translocation of chromosomal passenger proteins also in mammals.

Our understanding of the biological function of the Cdc14 family of dual specificity phosphatases in human cells is limited, in particular due to the difficulty in identifying specific substrate molecules of the individual Cdc14 family members. Here we describe a genetic approach based on a modified yeast two-hybrid system to identify novel substrates of hCdc14A. We report the identification and characterization of RN-tre, a GTPase-activating protein (GAP) for the Rab5 GTPase. We show that RN-tre preferentially forms a stable complex with a catalytically inactive C278S form of hCdc14A in human cells. We also show that RN-tre is regulated by cell cycle-dependent phosphorylation probably mediated by Cdk, and mutational analysis reveals that RN-tre phosphorylation is important for efficient binding to the catalytic site of hCdc14A. We furthermore show that hCdc14A phosphatase activity triggers the dephosphorylation of RN-tre *in vitro* as well as in human cells. Collectively, our experiments demonstrate that RN-tre is a novel physiological substrate of hCdc14A. Finally, we present *in vitro* evidence that points to a role of RN-tre phosphorylation in regulation of its GAP activity.

EXPERIMENTAL PROCEDURES

Cell Culture and Transfection—Human U2-OS osteosarcoma cells, HeLa cells, and 293T cells were grown in Dulbecco's modified Eagle's medium with 10% fetal bovine serum supplemented with 100 units/ml penicillin and 100 μg/ml streptomycin. Cells were transfected using FuGene 6 (Roche Applied Science) or Lipofectamine (Invitrogen) according to the manufacturer's instructions.

For double thymidine block, cells were grown in the presence of 2.5 mM thymidine (Sigma) for 16 h. Cells were washed in warm phosphate-buffered saline (PBS) and released in fresh media for 9 h, before a second thymidine block was initiated for 14 h. Cells were synchronized in S phase by treatment with 0.1 mM hydroxyurea (Sigma) for 23 h. To synchronize cells in mitosis, cells were treated with nocodazole (Sigma) at a final concentration of 40 ng/ml for 16 h. For the nocodazole washout experiments, the drug was removed by three washes in warm PBS, and cells were collected at various time points after release. To obtain mitotic cells without the use of drugs, U2-OS cells were partly synchronized by growth inhibition, trypsinized, and released into the cell cycle by dilution in fresh media. After 24–30 h, mitotic cells were collected by shake-off.

RNA interference in U2-OS cells was performed using siGENOME SMART pool siRNA oligonucleotides for Cdc14A (Dharmacon) or siRNA against Hsp70 as control. Cells were transfected using Oligofectamine (Invitrogen) according to the manufacturer's instructions, and cells were harvested after 48 h. Treatment of cells with roscovitine (Calbiochem) was performed using a final concentration of the inhibitor of 25 μM for 3 h at 37 °C. Cell cycle distribution by DNA content was analyzed by a FACSCalibur flow cytometer in cells fixed in 70% ethanol after staining with 0.1 mg/ml propidium iodide.

Yeast Two-hybrid Screen—A yeast two-hybrid screen was carried out using the GAL4-based system (31). The yeast strains CG1945 (MATa *Gal4-542 Gal80-538 ade2-101 His3-200 Leu2-3,-112 Trp1-901 Ura3-52 Lys2-801 URA3::GAL4 17mers (X3)-CyCITATA-LacZ LYS2::GAL1UAS-GAL1TATA-HIS3*

CYH^R) and Y187 (MATα *Gal4*Δ *Gal80*Δ *ade2-101 His3 Leu2-3,-112 Trp1-901 Ura3-52 URA3::UASGAL1-LacZ Met*$^-$) were used in all assays. Y187 cells were transformed with a human liver cDNA library (Clontech). Selection of positive diploids was made upon activation of the *HIS3* and *lacZ* reporter genes. Qualitative *lacZ* assays were performed by the filter lift X-gal method, and quantitative liquid β-galactosidase assays were performed as described in the manual from Clontech. Yeast media and genetic procedures were performed as described previously (32).

Plasmids—Plasmids HA2 RN-tre pcDNA4/TO and HA2 RN-tre pcDNA3.1 were used for transient expression of N-terminally HA-tagged RN-tre. The RN-tre open reading frame was amplified by PCR and inserted into pcDNA4/TO and pcDNA3.1 vectors (Invitrogen), respectively. Next, a PCR fragment encoding two HA tags was inserted just upstream and in frame with the RN-tre start codon.

To generate the HA2 RN-tre M13 pcDNA4/TO and HA2 RN-tre M13 pcDNA3.1 plasmids for transient expression of a phosphorylation site mutant form of RN-tre, a series of recombinant PCRs was performed to introduce the following mutations: S396A, S415A, T424A, S576A, S585A, S595A, S642A, S655A, S659A, S680A, S784A, S791A, and S798A. Details are available upon request. The mutant RN-tre open reading frame was cloned into pcDNA4/TO or pcDNA3.1 harboring two N-terminal HA epitopes.

The plasmid pEGFP-RN-tre encoding N-terminally GFP-fused RN-tre was described previously (33). The plasmid pEGFP-RN-tre M13, encoding N-terminally GFP-fused RN-tre carrying the phosphorylation site mutations, was generated by introducing the mutagenic PCR fragment into the pEGFP-C1 (Clontech) vector.

RN-tre-(447–828) pMAL-c2X was used to express the C-terminal domain of RN-tre fused at the N terminus to a maltose-binding protein. The plasmid was constructed by PCR amplification of the region corresponding to residues 447–828, which was inserted into the pMAL-c2X vector (New England Biolabs).

To produce GST fusion proteins GST RN-tre-(1–446) and GST RN-tre-(580–828), plasmids pGEX20T RN-tre-(1–446) and pGEX20T RN-tre-(580–828) were constructed by cloning the respective PCR-generated RN-tre fragments into the pGEX20T plasmid.

For two-hybrid analysis, sequences corresponding to Cdc14A, Cdc14A C278S, Cdc14B, and Cdc14B C314S were generated by PCR and cloned into the pAS2ΔΔ bait vector (Clontech). A fragment of RN-tre spanning residues 447–828 was cloned into the prey pACTII vector (Clontech). A similar fragment carrying the mutations S576A, S585A, S595A, S642A, S655A, S659A, S680A, S784A, S791A, and S798A was cloned into pACTII.

GFP-based expression plasmids of human Cdc14A wild type (WT) and C278S phosphatase-dead (PD) were engineered by inserting the respective PCR-derived fragments into the pEGFP-C1 (Clontech) vector. Plasmids expressing His_6Myc-tagged versions of Cdc14A WT and Cdc14A PD were constructed by cloning the respective Cdc14A sequences into the parental His_6Myc pcDNA3.1 vector obtained from Dr. P. Jackson. To generate the GFP-tagged Cdc14B, a PCR fragment spanning the Cdc14B open reading frame was inserted into the pEGFP-C1 vector (Clontech).

Plasmids pEGFP-C1 Cdc25B, pcDNA3 Myc-Aurora A, pBI-Cdk2/cyclin A, and pcDNA3 Myc-E2F4 were gifts from Dr. J. Lukas. Plasmids pcDNA3 Cdk1wt and Cdk1AF were generous gifts from Dr. M. Brandeis and Dr. S. Lev. All plasmids were subjected to sequencing to verify their integrity.

Antibodies—Antibodies used in this study include rabbit polyclonal anti-GAL4 DBD (sc-577; Santa Cruz Biotechnology, Inc., Santa Cruz, CA), mouse monoclonal anti-HA-conjugated agarose beads (sc-7392; Santa Cruz Biotechnology), rabbit polyclonal anti-HA Y11 (sc-805; Santa Cruz Biotechnology), mouse monoclonal anti-9E10 (sc-40; Santa Cruz Biotechnology), mouse monoclonal anti-Cdk7 (Danish Cancer Society), mouse monoclonal anti-RN-tre (39), rabbit monoclonal anti-phospho-MAPK/Cdk (catalog number 2325; Cell Signaling), mouse monoclonal anti-MCM7 (DCS14; Danish Cancer Society), rabbit polyclonal anti-Cdc25C (sc-327; Santa Cruz Biotechnology), rabbit polyclonal anti-Cdc27 (C-19; Santa Cruz Biotechnology), mouse monoclonal anti-GFP (sc-9996; Santa Cruz Biotechnology), mouse monoclonal anti-GST (sc-138; Santa Cruz Biotechnology), mouse monoclonal anti-cyclin B1 (sc-245; Santa Cruz Biotechnology), anti-goat polyclonal anti-Cdc14A (sc-25952; Santa Cruz Biotechnology), and mouse monoclonal anti-γ-tubulin (Santa Cruz Biotechnology).

Immunofluorescence and Microscopy—Cells grown on glass coverslips were fixed in ice-cold 1:1 (v/v) methanol/acetone for 7 min at room temperature. Coverslips were immunostained with antibodies specified in figure legends followed by DNA staining with ToPro3. Fluorescence- conjugated secondary antibodies were from Molecular Probes, Inc. (Carlsbad, CA). Confocal images were captured using a Zeiss 510 laser-scanning microscope (Carl Zeiss Microimaging Inc.) and processed using Adobe Photoshop 8.0.

Lysate Preparation and Immunoblotting—Cells were lysed in Nonidet P-40 buffer (50 mM Tris-HCl, pH 7.5, 125 mM NaCl, 0.5% Nonidet P-40) containing 1 mM DTT, 5 μg/ml leupeptin, 2 μg/ml aprotinin, 0.1 mM phenylmethylsulfonyl fluoride, 10 mM β-glycerophosphate, 1 mM NaF, and 0.1 mM Na_3VO_4, and lysates were cleared by centrifugation at 20,000 rpm for 15 min. Proteins were transferred to nitrocellulose membrane with a semidry electrophoresis transfer apparatus and probed with the indicated antibodies according to the manufacturer's instructions. Blots were developed using the ECL system (Amersham Biosciences).

Immunoprecipitation, Kinase Assays, and Phosphatase Assays—Co-immunoprecipitation experiments involving HA-tagged RN-tre were performed with 1 mg of cell extract. Extract was precleared for 30 min at 4 °C with 20 μl of protein G-Sepharose beads (50% slurry) and subsequently incubated with 6 μl (3 μg) of HA-conjugated agarose beads (HA-probe F-7 AC; Santa Cruz Biotechnology) for 1.5 h at 4 °C. Samples were washed four times with 1 ml of Nonidet P-40 buffer, and the beads were boiled in 2× Laemmli sample buffer (LSB) for 5 min prior to SDS-PAGE. Co-immunoprecipitation experiments on endogenous proteins were performed with 1–2 mg of cell extract and 4.5 μg of mouse monoclonal anti-RN-tre antibody coupled to

protein G-Sepharose beads using a similar method. To cross-link proteins prior to cell extraction, cells were washed twice in cold PBS and incubated on ice for 10 min in 1% formaldehyde (diluted in PBS). The reaction was stopped by incubation with 0.1 M glycine base for 5 min. Cells were rinsed twice with PBS and lysed with Nonidet P-40 buffer as outlined above.

For *in vitro* kinase assays, mitotic Cdk1-cyclin B complexes were immunopurified from 250 μg of extract derived from nocodazole-arrested cells using 0.2 μg of mouse monoclonal anti-cyclin B antibody and 40 μl of protein G-Sepharose beads. After a 1-h incubation at 4 °C, the beads were washed three times with Nonidet P-40 buffer and two times with kinase buffer (50 mM Hepes, pH 7.5, 10 mM $MgCl_2$, 2.5 mM EGTA) containing 1 mM DTT, 10 mM β-glycerophosphate, 1 mM NaF, and 0.1 mM Na_3VO_4. 5 μg of GST or GST-RN-tre substrate was added in kinase buffer containing 1 μl of [γ-^{32}P]ATP (10 μCi/μl) and 0.1 M cold ATP. The reaction was incubated at 30 °C for 30 min and stopped by boiling in 4× LSB for 5 min.

To perform the kinase reaction directly in extract, 5 μg of GST or GST-RN-tre prebound to GSH resin was incubated with 50 μg of extract from exponentially growing cells or mitotic cells in a total volume of 25 μl of kinase buffer containing 1 μl of [γ-^{32}P]ATP (10 μCi/μl) and 0.1 mM cold ATP. After a 30-min incubation at 30 °C, the resin was washed four times in Nonidet P-40 buffer and boiled in 2× LSB for 5 min prior to SDS-PAGE on 12% protein gels. Where indicated, extract was preincubated with 10 or 25 μM roscovitine for 20 min on ice prior to incubation with GSH resin. Purified Cdc2 (Cdk1-cyclin B) kinase was purchased from New England Biolabs and used according to the manufacturer's instructions.

For *in vitro* phosphatase assays, endogenous RN-tre was immunopurified from 1 mg of mitotic extract and washed three times with Nonidet P-40 buffer followed by three washes with phosphatase buffer (50 mM imidazole, pH 7.5, 50 mM NaCl, 1 mM EDTA) containing 1 mM DTT, 5 μg/ml leupeptin, 2 μg/ml aprotinin, and 0.1 mM phenylmethylsulfonyl fluoride. The phosphatase reaction was performed at 30 °C for 30 min in phosphatase buffer in the presence of 5 μg of bacterially produced GST Cdc14A WT, GST Cdc14A PD or alkaline phosphatase (10 units) or left untreated. Samples were boiled in 4× LSB for 5 min prior to analysis.

Recombinant Protein Production and in Vitro GSH Resin Pull-down Assays—Production of recombinant GST-Cdc14A WT, GST-Cdc14A PD, GST-RN-tre-(1–447), and GST-RN-tre-(580–828) in *Escherichia coli* strain BL21 was performed as described (32). GST fusion proteins were purified from bacterial lysates on GSH-Sepharose resin (Amersham Biosciences) according to the manufacturer's instructions and dialyzed before use. Recombinant maltose-binding protein-RN-tre-(447–828) was similarly produced in BL21 cells and purified from bacterial lysates on an amylose column (New England Biolabs) followed by dialysis as specified by the manufacturer.

In vitro translation of RN-tre was performed using the TNT Quick Coupled Transcription/Translation System from Promega according to the manufacturer's instructions. *In vitro* translated RN-tre was used as a substrate in a "cold" *in vitro* kinase assay reaction using Cdk1-cyclin B immunopurified from mitotic cells. After the kinase reaction, the *in vitro* translated RN-tre substrate was separated from the beads, and phosphorylation was verified as a mobility shift after SDS-PAGE.

For the RN-tre and Cdc14A *in vitro* binding assay, 5 μg of GST or GST-Cdc14A PD was immobilized on 25 μl of GSH resin and incubated for 20 min in ELB binding buffer (50 mM Hepes, pH 7.0, 250 mM NaCl, 5 mM EDTA, 0.1% Nonidet P-40 + 1 mM DTT, 5 μg/ml leupeptin, 2 μg/ml aprotinin, and 0.1 mM phenylmethylsulfonyl fluoride) in the presence or absence of increasing amounts of sodium tungstate (Sigma). 5 μl of phosphorylated *in vitro* translated RN-tre protein was added, and the mixture was incubated for 1 h at 4 °C. Samples were washed five times with 1 ml of ELB binding buffer, and resin was boiled in 4× LSB before SDS-PAGE.

Orthophosphate Labeling and Two-dimensional Electrophoresis—U2-OS cells transiently expressing HA RN-tre WT or HA RN-tre M13 were labeled for 3 h in phosphate-free Dulbecco's modified Eagle's medium with 20 mM Hepes, pH 7.2, 10% dialyzed serum, and 1 mCi/ml [^{32}P]orthophosphate (PBS43; Amersham Biosciences). Cells were lysed in radioimmune precipitation buffer (20 mM Tris-HCl, pH 8.0, 150 mM NaCl, 1% Nonidet P-40, 0.5% deoxycholate, 0.1% SDS) and processed for immunoprecipitation. Two-dimensional phosphopeptide mapping and phosphoamino acid analysis were performed as described (34). Tryptic phosphopeptides were separated on thin layer cellulose plates using a Hunter thin layer electrophoresis system (HTLE-7000; 2000 V for 25 min), followed by chromatography in the second dimension (isobuturic acid buffer).

Biochemical GAP Assays—GAP assays were performed using the filter binding method described in Ref. 35. Briefly, purified recombinant Rab5 (20 nmol) was preloaded with 2 μl of [γ-^{32}P]GTP (10 mCi/ml, 5000 Ci/mmol) in 100 μl of buffer (25 mM Tris-HCl, pH 7.6, 50 mM NaCl, 5 mM EDTA, 0.1 mM DTT) for 20 min at 30 °C. $MgCl_2$ was added to a final concentration of 20 mM, and the GTPase was incubated at 30 °C for an additional 5 min and stored on ice.

Total cellular lysates (5 mg) from HeLa cells growing or synchronized at prometaphase with 50 ng/ml nocodazole (Sigma) for 14 h were immunoprecipitated with the mouse monoclonal anti-RN-tre antibody. Total cellular lysates (3 mg) from 293T cells transiently transfected for 24 h with HA-RN-tre WT, HA-RN-tre M13, or empty vector were immunoprecipitated with the anti-HA antibody. In both cases, total cellular lysates were obtained with lysis buffer (25 mM Tris-HCl, pH 7.6, 100 mM NaCl, 1% glycerol, 1 mM $MgCl_2$, 1 mM EDTA, 1 mM DTT + protease inhibitor mixture (Calbiochem)). Immunoprecipitates were washed three times with lysis buffer and three times with GAP buffer and incubated with [γ-^{32}P]GTP-loaded Rab5 (2 μM) diluted in GAP buffer (25 mM Tris-HCl, pH 7.6, 0.1 M NaCl, 11 mM $MgCl_2$, 1 mM DTT). Aliquots corresponding to time point 0 were taken. Reactions were then incubated at 30 °C, and aliquots were taken at time points indicated in the figure legend, diluted in 2.5 ml of ice-cold washing buffer (50 mM Tris-HCl, pH 7.6, 50 mM NaCl, 20 mM $MgCl_2$), and filtered through prewetted nitrocellulose filters. Filters were washed with 5 ml of cold washing buffer, dried, and counted in 5 ml of scintillation counting medium (Filter-count; Packard) with Liquid Scintillation Analyzer Tri-carb 2100TR (Packard).

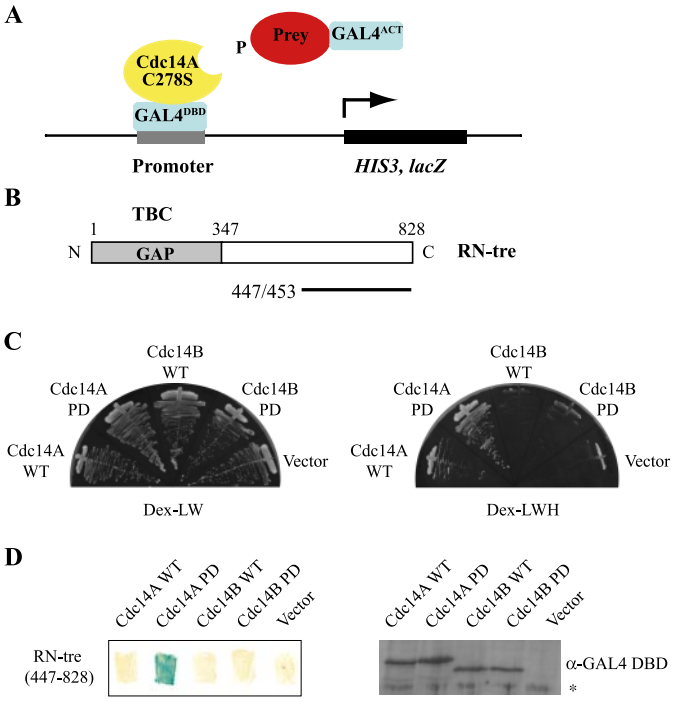

FIGURE 1. **RN-tre interacts with the hCdc14A C278S phosphatase-dead mutant in a two-hybrid screen.** *A*, a schematic representation of the yeast substrate trapping system. Stable complex formation between phosphorylated prey proteins fused to the GAL4 activation domain (*ACT*)- and the GAL4 DNA-binding domain (*DBD*)-fused hCdc14A bait carrying a catalytically inactive C278S mutation will lead to activation of transcription of the reporter genes *HIS3* and *lacZ*. *B*, RN-tre contains a TBC domain encoding a GAP for the Rab5 GTPase in the N-terminal region. The regions in the C terminus involved in Cdc14A binding are indicated below. *C*, specificity of RN-tre interaction. Y187 yeast cells, expressing the prey RN-tre-(447–828), were mated with CG1945 cells expressing the indicated Cdc14 baits, and diploid cells were tested for growth on media lacking histidine. *D*, the strains from *C* were grown on selective media and examined by the qualitative filter lift X-gal assay, where *blue* color development is indicative of strong interaction (*left*). Expression of the GAL4-DBD fusion proteins was analyzed by immunoblotting of yeast extracts using the anti-GAL4 DBD antibody (*right*). Nonspecific protein recognized by the antibody is indicated with an *asterisk*.

TABLE 1

Interaction between RN-tre-(447–828) and various GAL4 fusions assayed as *lacZ* reporter gene activity

CG1945/Y187 diploid yeast cells expressing the indicated fusion proteins were grown in synthetic medium lacking tryptophan and leucine. β-Galactosidase activity was then measured using *o*-nitrophenyl-β-D-galactoside as a substrate. β-Galactosidase activities (in Miller units) are presented in mean values ± S.D. obtained with three independent transformants.

GAL4 fusion	Activation domain fusion	β-Galactosidase activity
		units
Cdc14A WT	RN-tre-(447–828)	0.13 ± 0.06
Cdc14A C278S	RN-tre-(447–828)	55.67 ± 2.31
Cdc14B WT	RN-tre-(447–828)	0.13 ± 0.06
Cdc14B C314S	RN-tre-(447–828)	0.18 ± 0.11
Cdc14A C278S	Vector	0.26 ± 0.05
Vector	RN-tre-(447–828)	0.23 ± 0.06
Vector	Vector	0.28 ± 0.07

RESULTS

A Genetic Substrate-trapping Screen for the Human Dual Specificity Phosphatase Cdc14A—To shed light on the biological function(s) of hCdc14A, we designed a genetic substrate-trapping method, which would allow us to identify physiological substrates of the phosphatase (Fig. 1*A*). This system is based on the conventional yeast two-hybrid screen with the single modification that an hCdc14A mutant harboring a substitution of the active site cysteine to serine (C278S) was employed as bait instead of the wild type protein. This mutation causes a complete loss of *in vitro* phosphatase activity (24). Although replacement of the active cysteine may induce local changes in the conformation of the catalytic site, which could affect the affinity for substrates (36), we reasoned that a catalytically inactive C278S mutation would allow a substrate complex formation sufficiently stable to withstand screening. Such a genetic strategy has previously been used successfully for identifying protein-tyrosine phosphatase substrates (37).

Screening of candidate clones was performed in two steps. Initially, we isolated 205 positive yeast clones from a human liver cDNA library (110×10^6 independent clones) by their ability to grow on selective media lacking histidine. These candidate clones were further examined for expression of the *lacZ* reporter gene, and positive clones after the second step screening (63) were sent for sequence analysis.

An interesting cDNA isolated with high frequency and with overlapping fragments encoded the C-terminal region of the RN-tre protein (Fig. 1*B*). RN-tre contains a TBC (for Tre2/Bub2/Cdc16) homology domain in the N terminus, which encodes a GAP for the Rab5 GTPase (33). Rab5 has a well defined role in regulating membrane trafficking in the early endocytic pathway (38) and is involved in control of actin cytoskeleton remodeling (39). Importantly, we observed that the C-terminal region of RN-tre was significantly impaired in the interaction with WT hCdc14A and failed to interact with the hCdc14B isoform even in a PD configuration, suggesting that RN-tre is a promising candidate for a specific hCdc14A target (Fig. 1, *C* and *D*, and Table 1).

Interaction of Cdc14A and RN-tre in Human Cells—To address whether hCdc14A forms a complex with RN-tre in human cells, we transiently expressed HA RN-tre in combination with Myc Cdc14A WT or Myc Cdc14A PD in U2-OS cells. Next, co-immunoprecipitation experiments were performed using either anti-HA-conjugated beads or IgG as control. As shown in Fig. 2*A*, immunoprecipitation of HA RN-tre resulted in retention of Myc Cdc14A PD but not Myc Cdc14A WT, although both Cdc14A forms were expressed at a similar level. As expected, comparable amounts of IgG failed to precipitate HA RN-tre or Myc Cdc14A. Reciprocal immunoprecipitation experiments produced similar results (data not shown).

Consistent with its function in intracellular trafficking, RN-tre localizes predominantly at the plasma membrane but is also detectable on intracellular membranes and in the cytosol (33, 39). Following ectopic expression of Myc Cdc14A PD, a pool of GFP-fused RN-tre is also found at the centrosome co-localizing with Myc Cdc14A PD and γ-tubulin (Fig. 2, *B* and *C*). Approximately 90% of the cells expressing the Myc Cdc14A PD protein showed accumulation of GFP RN-tre at the centrosome compared with less than 5% in cells expressing the Myc Cdc14A WT enzyme (Fig. 2*C*). Thus, the preferential trapping of RN-tre by a catalytically inactive Cdc14A mutant in human cells is strongly indicative of an enzyme/substrate association.

If RN-tre interacts with wild type Cdc14A in a transient and highly dynamic fashion, we reasoned that we might detect RN-tre and Cdc14A together if protein complexes were immobi-

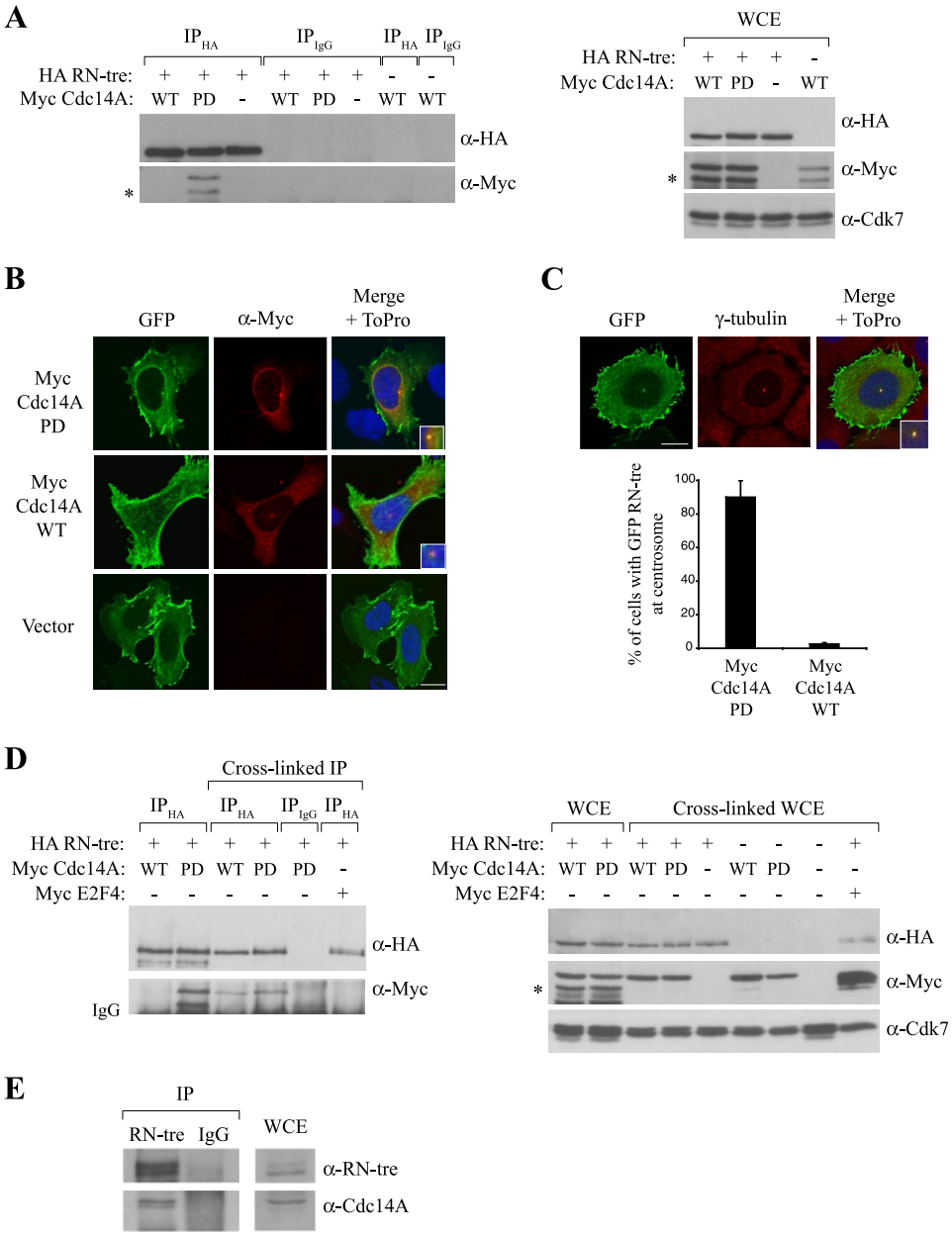

FIGURE 2. **RN-tre forms a complex with Cdc14A in human cells.** *A*, U2-OS cells were co-transfected with HA RN-tre and the indicated Myc Cdc14A expression plasmids. Cells were harvested after 21 h, lysates were subjected to immunoprecipitation using mouse monoclonal anti-HA antibody or nonspecific mouse IgG, and precipitated proteins were detected with rabbit polyclonal anti-HA and mouse monoclonal anti-Myc (9E10) antibodies. Whole cell extract (*WCE*) samples are shown to the *right*. Myc Cdc14A-derived degradation product is indicated with an *asterisk*. Cdk7 serves as a loading control. *B*, confocal analysis of U2-OS cells expressing GFP-RN-tre and the indicated Myc Cdc14A proteins, stained with the mouse monoclonal anti-Myc (9E10) antibody (*red*). *Merged images* are also shown (*blue*, ToPro nuclear stain). Co-localization of GFP and Myc signal is shown in *yellow* in the *merged image*. The centrosomal region is magnified in the *inset*. *Scale bar*, 10 μm unless otherwise stated. *C*, cells from *B* were stained for γ-tubulin (*red*). A representative cell showing co-localization of GFP RN-tre and γ-tubulin is shown at the *top*. Shown is quantification of cells with GFP RN-tre signal at the centrosome. Co-transfection efficiency of plasmids in each case was >95% (data not shown). Mean values ± S.D. ($n = 3$, >200 cells scored for each sample) are shown. *D*, U2-OS cells were co-transfected with HA RN-tre and Myc expression plasmids for 21 h. Where indicated, proteins were cross-linked prior to cell extraction. Lysates were immunoprecipitated as indicated, and the precipitated proteins were detected with mouse anti-HA and mouse anti-Myc (9E10) antibodies. Whole cell extract (*WCE*) samples are shown to the *right*. Myc Cdc14A-derived degradation product is indicated with an *asterisk*. Cdk7 serves as a loading control. *E*, endogenous RN-tre was immunoprecipitated from exponentially growing U2-OS cells after cross-linking using the mouse monoclonal anti-RN-tre antibody or mouse IgG. Immunostaining was performed with mouse monoclonal anti-RN-tre antibody and goat polyclonal anti-Cdc14A antibody.

lized by mild formaldehyde cross-linking prior to lysate preparation and immunoprecipitation. As shown in Fig. 2*D*, this approach allowed HA-RN-tre to retain Myc Cdc14A WT, in addition to Cdc14A PD, on the HA-conjugated beads. Under similar conditions, HA RN-tre failed to co-precipitate the unrelated Myc E2F4 protein, which served as a control, verifying that the cross-linking solely acts on proteins in close proximity.

Finally, we examined if endogenous RN-tre and Cdc14A form a complex in human cells. As shown in Fig. 2*E*, co-immunoprecipitation experiments on cross-linked extracts derived from exponentially growing U2-OS cells revealed that Cdc14A co-purifies with RN-tre, arguing that the two proteins indeed interact *in vivo*. In agreement, gel filtration experiments using U2-OS cell lysates showed that RN-tre co-eluted with hCdc14A containing fractions (data not shown).

RN-tre Is Regulated by Cell Cycle-dependent Phosphorylation, Which Can Be Antagonized by hCdc14A—Consistent with the notion that RN-tre is a potential substrate of hCdc14A, biochemical analysis showed that it is modified by phosphorylation during the cell cycle. RN-tre protein displays a prominent mobility shift when immunopurified from cells synchronized in mitosis by nocodazole treatment compared with RN-tre purified from either exponentially growing cells or cells synchronized in G_1/S by double thymidine block or S phase by hydroxyurea treatment (Fig. 3*A*). Immunostaining with an antibody that specifically recognizes serine residues phosphorylated by MAPK/Cdk kinases confirmed that the mobility shift of RN-tre is caused by phosphorylation, in particular during mitosis (Fig. 3*A*).

We next examined the kinetics of RN-tre dephosphorylation after U2-OS cells synchronized in prometaphase by nocodazole treatment were released into the cell cycle following drug removal (Fig. 3*B*). RN-tre phosphorylation rapidly disappears as cells exit mitosis coincident with mitotic Cdk inactivation visualized by the dephosphorylation of Cdc25C and Cdc27 (Fig. 3*B*). Importantly, the mitotic phosphorylation is not a consequence of nocodazole exposure, since analysis of

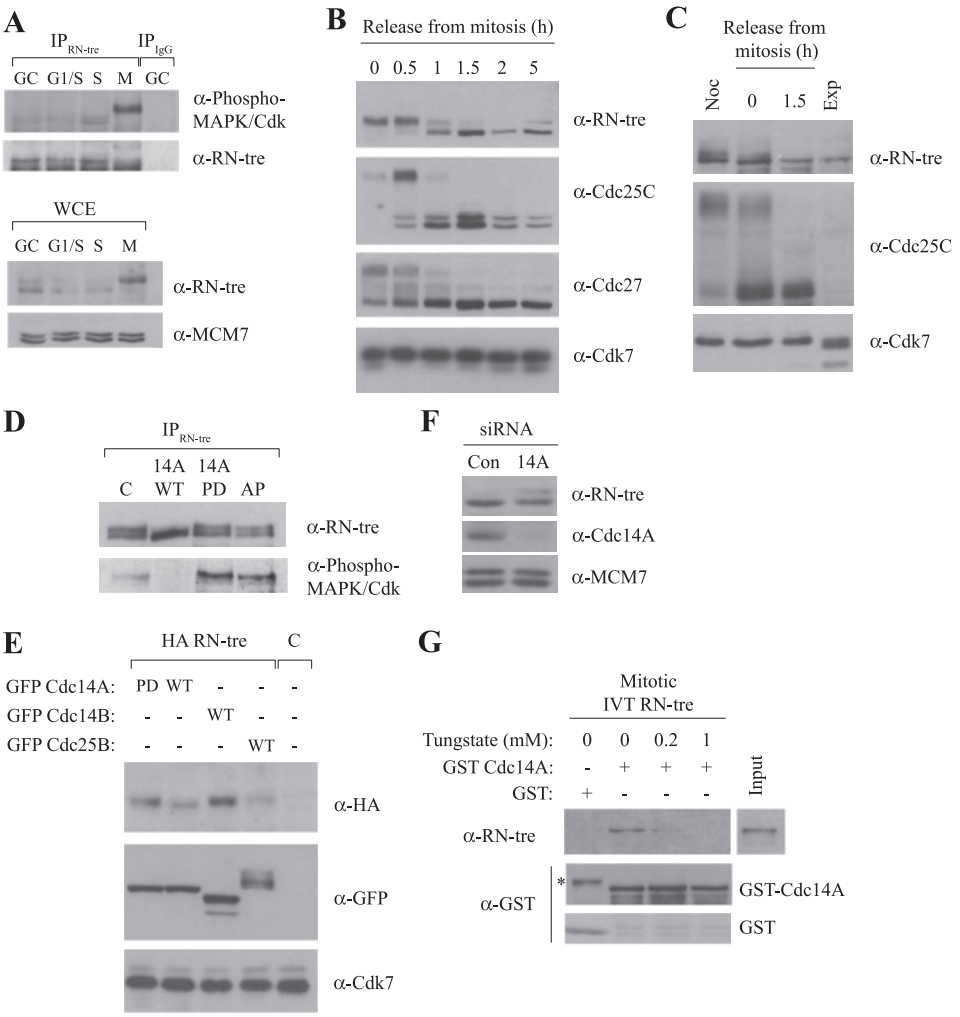

FIGURE 3. **RN-tre is regulated by cell cycle-dependent phosphorylation.** *A*, endogenous RN-tre protein was immunoprecipitated from U2-OS cells growing (*GC*) or synchronized at G_1/*S* by double thymidine block (*G1/S*), at S by hydroxyurea treatment (*S*), or at mitosis by nocodazole block (*M*), using the mouse monoclonal anti-RN-tre antibody or IgG. The precipitates were analyzed using the anti-phospho-MAPK/Cdk antibody and the anti-RN-tre antibody. MCM7 serves as a loading control. *B*, U2-OS cells were synchronized at mitosis by nocodazole treatment for 16 h. Cells were released by drug removal, and samples were collected at different time points after release for Western blot analysis with the indicated antibodies and fluorescence-activated cell sorting analysis (data not shown). *C*, U2-OS cells were partly synchronized in G_1 by growth to confluence, digested with trypsin, and released by diluting in fresh media. After 24 h, mitotic cells were collected by shake-off, and samples were examined at the indicated time points for Western blot analysis and fluorescence-activated cell sorting (not shown). *D*, endogenous RN-tre protein was immunopurified from U2-OS cells synchronized at mitosis by nocodazole using the mouse monoclonal anti-RN-tre antibody. The precipitate was equally divided into four samples and used in a phosphatase reaction with purified GST Cdc14A WT (*14A WT*), GST Cdc14A PD (*14A PD*), or alkaline phosphatase (*AP*) or left untreated (*C*). Samples were subsequently examined by 8% SDS-PAGE and immunostaining with the indicated antibodies. *E*, U2-OS cells expressing HA-RN-tre in combination with the indicated GFP-fused phosphatases were harvested 21 h after transfection, and extracts were analyzed by immunoblotting with the indicated antibodies. Co-transfection efficiency in all cases was >95% (data not shown). *F*, U2-OS cells were silenced with control oligonucleotides (*Con*) or with Cdc14A siRNA oligonucleotides (*14A*) for 48 h. Cell lysates were analyzed by immunoblotting as indicated. *G*, GST-Cdc14APD or GST alone was bound to GSH resin and incubated in the presence or absence of increasing concentrations of sodium tungstate for 20 min. *In vitro* translated RN-tre phosphorylated *in vitro* by Cdk1-cyclin B (*Mitotic IVT RN-tre*) was added to the reaction and incubated for 1.5 h at 4 °C. After extensive washing, the GSH beads were boiled in 2× LSB, and bound proteins were analyzed by immunostaining with the mouse monoclonal anti-GST antibody and with the mouse monoclonal anti-RN-tre antibody. *Input* shows the amount of *in vitro* translation RN-tre used in the reaction. An *asterisk* indicates a nonspecific band in the GST sample. *Noc*, nocodazole; *Exp*, exponential.

mitotic cells collected in the absence of drugs shows a comparable shift in RN-tre protein mobility (Fig. 3*C*).

To determine if hCdc14A is a functional phosphatase for RN-tre, we initially tested if Cdc14A can dephosphorylate RN-tre *in vitro*. Treatment of RN-tre immunoprecipitates prepared from mitotically arrested cells with purified GST-Cdc14A resulted in a collapse of the low mobility forms of RN-tre into a single band and, importantly, resulted in loss of recognition by the anti-phospho-MAPK/Cdk antibody. In contrast, RN-tre phosphorylation was not greatly affected by either the catalytically inactive version of Cdc14A (GST-Cdc14PD) or alkaline phosphatase (*AP*) (Fig. 3*D*). Thus, hCdc14A is capable of dephosphorylating RN-tre on serine residues *in vitro*.

We next examined if hCdc14A dephosphorylates RN-tre *in vivo*. U2-OS cells were transiently transfected with HA-RN-tre in combination with different GFP-fused phosphatases belonging to the protein-tyrosine phosphatase family (Fig. 3*E*). Indeed, expression of GFP Cdc14A WT but not its catalytically inactive counterpart reduced the mobility of HA RN-tre by SDS-PAGE, indicative of its dephosphorylation, even detectable in exponentially growing cells. Although phosphatases often are considered to be promiscuous (40), expression of GFP-Cdc14B or GFP-Cdc25B did not affect RN-tre mobility, suggesting that Cdc14A may be the critical phosphatase dephosphorylating RN-tre in human cells (Fig. 3*E*). In support, we found that depletion of Cdc14A by siRNA in U2-OS cells, which did not increase the mitotic index (data not shown), resulted in accumulation of phosphorylated RN-tre as judged by a decrease in RN-tre protein mobility (Fig. 3*F*).

To corroborate that Cdc14A is a regulator of RN-tre, we analyzed the ability of Cdc14A to bind directly to RN-tre and the involvement of the active site region. Purified GST-Cdc14A PD or GST alone as control was immobilized on GSH resin and subsequently incubated with phosphorylated *in vitro* translated RN-tre (see "Experimental Procedures" for details). Indeed, we found that GST-Cdc14A PD binds directly to phosphorylated RN-tre (Fig. 3*G*). We next used sodium tungstate, a known competitive inhibitor of protein-tyrosine phosphatases, including Cdc14 (41), which binds the active site in a manner

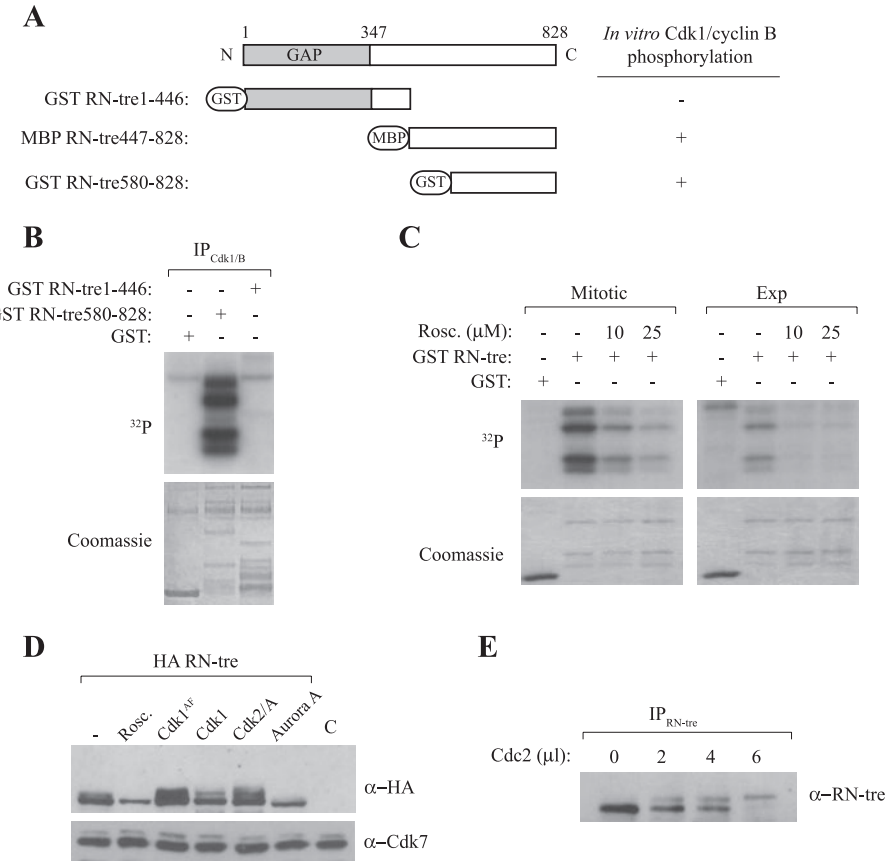

FIGURE 4. **RN-tre is a substrate of cyclin-dependent kinases *in vitro* and *in vivo*.** *A*, schematic representation of RN-tre substrates fused to GST or maltose-binding protein used in kinase reactions *in vitro* with Cdk1-cyclin B kinase. *B*, Cdk1-cyclin B kinase was immunopurified from mitotic extract using the mouse monoclonal anti-cyclin B antibody and incubated with the GST-RN-tre substrates in the presence of [γ-^{32}P]ATP. Samples were analyzed by 12% SDS-PAGE followed by Coomassie staining and autoradiography (*C*). GST-RN-tre-(580–828) (*GST RN-tre*) or GST alone was used in a kinase reaction with mitotic extract or extract from exponentially growing cells. The indicated samples were pretreated with increasing amount of roscovitine prior to kinase reaction. Samples were analyzed as in *B*. *D*, U2-OS cells expressing HA-RN-tre in combination with indicated kinases were harvested after 21 h, and extract was analyzed by immunoblotting with the indicated antibodies. Co-transfection efficiency was comparable in all cases (data not shown). *E*, endogenous RN-tre protein was immunoprecipitated from growing U2-OS cells, and the precipitate was divided into equal aliquots, which were phosphorylated *in vitro* using increasing amounts of purified Cdc2 kinase (20 units/ml). The samples were analyzed by 8% SDS-PAGE and immunostained with the mouse monoclonal anti-RN-tre antibody.

similar to the phosphate of substrates to assess if the active site is required for RN-tre binding. Pretreatment of immobilized GST-Cdc14A PD with sodium tungstate reduced the binding to RN-tre in a concentration-dependent manner (Fig. 3*G*), suggesting that RN-tre binds Cdc14A via its active site. Collectively, our data strongly suggest that RN-tre is a novel physiological substrate of Cdc14A in human cells.

RN-tre Phosphorylation Status Is Modulated by Cdk Activity—Since mitotic RN-tre is phosphorylated at sites recognized by an anti-phospho-MAPK/Cdk antibody (Fig. 3*A*) and Cdk1 is the most prominent kinase in mitosis, we wanted to examine the possibility that Cdk1 phosphorylates RN-tre during mitosis. Initially, we tested if Cdk1 could mediate RN-tre phosphorylation *in vitro*. A panel of RN-tre fragments fused to GST or maltose-binding protein was incubated with Cdk1-cyclin B complexes purified from mitotic cells in the presence of [γ-^{32}P]ATP (Fig. 4, *A* and *B*). C-terminal fragments of RN-tre corresponding to residues 447–828 and 580–828 were strongly phosphorylated by Cdk1 *in vitro*, whereas the N-terminal fragment spanning residues 1–446 and GST alone were poor substrates.

Kinase reactions using GST-RN-tre-(580–828) as substrate were also performed under more physiological conditions directly in extract derived from mitotic or exponentially growing cells. We observed that phosphorylation of GST-RN-tre-(580–828) was enhanced in the mitotic extract, consistent with mitotic activation of Cdk1 (Fig. 4*C*). Incorporation of radiolabel was significantly reduced after preincubating the extracts with roscovitine, a potent Cdk inhibitor, suggesting that Cdk is the major kinase contributing to RN-tre phosphorylation *in vitro* (Fig. 4*C*).

Next, we examined the effects of modulating Cdk activity on RN-tre phosphorylation *in vivo*. Overexpression of wild type Cdk1 or Cdk1AF (a constitutive active form of Cdk1) both resulted in a mobility shift of HA RN-tre (Fig. 4*D*). Overexpression of the related Cdk2 kinase in complex with cyclin A also induced phosphorylation of HA RN-tre (Fig. 4*D*), consistent with our observations that this kinase complex also phosphorylated RN-tre *in vitro* (data not shown). Other mitotic kinases, such as Aurora A (Fig. 4*D*), Nek2, and Mps1, did not affect RN-tre phosphorylation status *in vivo* (data not shown). In contrast, treatment of HA RN-tre-expressing cells with the Cdk inhibitor roscovitine led to a reduction in RN-tre protein mobility indicative of loss of phosphorylation (Fig. 4*D*). Taken together, our data suggest that Cdk (and presumably Cdk1) is responsible for RN-tre phosphorylation at mitosis. In support, we observed that phosphorylation by purified Cdc2 kinase (Cdk1-cyclin B) of RN-tre immunopurified from exponentially growing cells is alone sufficient to induce a substantial RN-tre mobility shift (Fig. 4*E*).

Mutation Analysis of Putative RN-tre Phosphorylation Sites—To determine the biological significance of RN-tre phosphorylation, we initiated a mutation analysis of putative Cdk consensus phosphorylation sites in RN-tre. Sequence analysis identified 16 putative phosphorylation sites corresponding to minimum Cdk phosphorylation sites (Ser/Thr-Pro), the majority of which were located in the C-terminal region. Since RN-tre is phosphorylated on serine residues in mitosis, we systematically mutated serine residues in these putative sites to nonphosphorylatable alanine residues. A collection of purified GST fusion proteins carrying a variety of mutant combinations were sub-

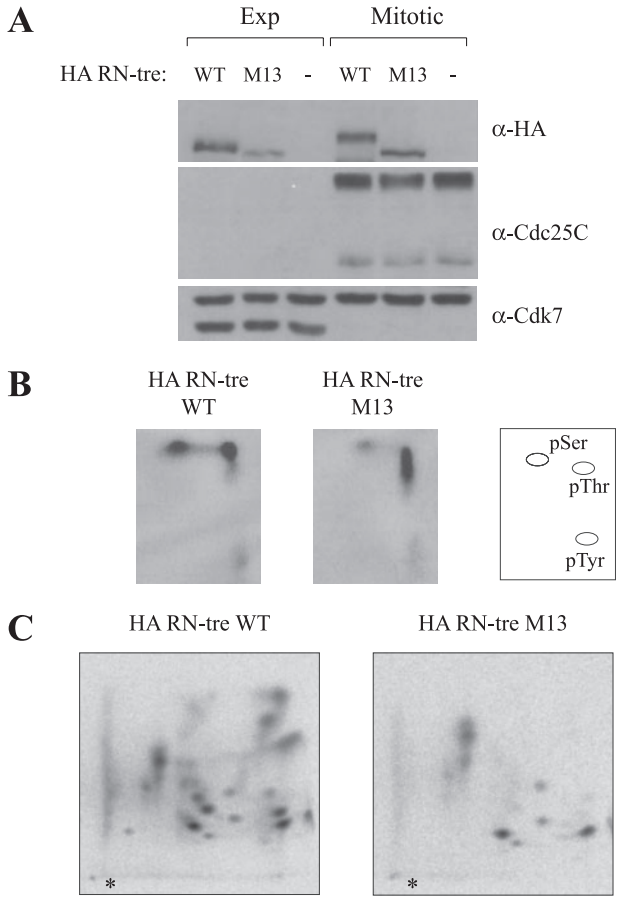

FIGURE 5. **Analysis of putative phosphorylation sites in RN-tre.** *A*, U2-OS cells were transiently transfected with HA-RN-tre WT or HA-RN-tre M13 expression plasmids and left untreated (*Exp*) or treated with nocodazole for 16 h to collect mitotic cells by shake-off (*Mitotic*) Cells were harvested, and extract was analyzed by immunoblotting as indicated. *B*, phosphoamino acid analysis performed on immunopurified HA-RN-tre WT or HA-RN-tre M13 from U2-OS cells subjected to *ortho*-phosphate labeling. Migration of phosphorylated serine (*pSer*), threonine (*pThr*), and tyrosine (*pTyr*) is indicated on the right. *C*, two-dimensional phosphopeptide mapping performed on HA-RN-tre WT and HA-RN-tre M13 proteins. *Asterisks* mark the site of origin.

jected to *in vitro* Cdk1-cyclin B kinase assays. To completely eliminate *in vitro* phosphorylation by this mitotic kinase complex, a total of 13 sites in RN-tre had to be substituted (data not shown).

We next analyzed the behavior of the RN-tre phosphorylation mutant (hereafter referred to as M13) after transient expression in U2-OS cells. Whereas the HA RN-tre wild type protein shows an increased phosphorylation in mitosis, evident as a substantial decrease in mobility after SDS-PAGE, the HA RN-tre M13 protein migrated as a single focused band even in mitotic extract (Fig. 5*A*). In addition, the RN-tre M13 mutant was no longer sensitive to increased Cdk levels (data not shown). To validate that phosphorylation is in fact impaired in the RN-tre M13 mutant, [^{32}P]orthophosphate labeling experiments were conducted with U2-OS cells expressing either HA RN-tre wild type or HA RN-tre M13 protein. RN-tre was immunopurified on HA-conjugated beads and subjected to phosphopeptide analysis. Although similar amounts of RN-tre were immunoprecipitated (not shown), phosphoamino acid analysis revealed that phosphorylation on serine residues was dramatically reduced in the M13 mutant (Fig. 5*B*). However, significant phosphorylation remained on threonine residues in both M13 and wild type protein, suggesting a complex phosphorylation regulation of RN-tre *in vivo*. In agreement, two-dimensional phosphopeptide mapping analysis confirmed that, although phosphorylation was reduced in the M13 mutant, several phosphopeptides were still present (Fig. 5*C*).

If Cdc14A recognizes and specifically binds phosphorylated RN-tre, one might predict that loss of RN-tre phosphorylation would impair complex formation. Indeed, we found that the RN-tre mutant carrying serine to alanine mutations had lost the ability to bind to the Cdc14A PD bait in the two-hybrid system (Fig. 6*A*; data not shown). Furthermore, co-immunoprecipitation experiments using transiently transfected U2-OS cells showed that the RN-tre M13 mutant, in contrast to the wild type protein, was unable to form a stable complex with Myc Cdc14A PD (Fig. 6*B*). The decreased ability of RN-tre M13 to interact with hCdc14A was also evident by the inability of Myc Cdc14A PD to retain GFP RN-tre M13 at the centrosome after their co-expression in U2-OS cells (Fig. 6*C*). Although serine to alanine substitutions are not predicted to have a large impact on the three-dimensional structure of the protein, we cannot exclude the possibility that the introduced mutations have altered the conformation of RN-tre and thereby its binding affinities. However, we favor the idea that phosphorylation of RN-tre is necessary for efficient recognition/binding to Cdc14A, which is in line with our biochemical data (Fig. 3*F*). The RN-tre M13 protein exhibits a subcellular localization similar to that of its wild type counterpart (Fig. 6*C*), which argues against major conformational changes in the mutant and, more importantly, provides evidence that serine phosphorylation does not greatly affect RN-tre distribution to the plasma membrane and intracellular membranes.

The GAP Activity of RN-tre Is Regulated by Phosphorylation—RN-tre displays GAP activity toward the Rab5 GTPase (33). This prompted us to explore the possibility that phosphorylation may influence the catalytic activity of RN-tre by using Rab5 as a "model" substrate. For this purpose, comparable amounts of immunopurified endogenous RN-tre from HeLa cell lysates derived from exponentially growing cells or nocodazole-arrested mitotic cells were examined in biochemical filter-binding GAP assays containing purified Rab5 preloaded with [γ-^{32}P]GTP. Samples were taken at indicated time points, and the amount of nonhydrolyzed [γ-^{32}P]GTP, which remained filter-bound, was counted. We reproducibly detected a higher [γ-^{32}P]GTP hydrolysis in RN-tre precipitates from mitotic cells compared with growing cells, suggesting that RN-tre has an increased GAP activity in mitosis (Fig. 7*A*).

To examine if the RN-tre mutant harboring serine to alanine substitutions has an altered GAP activity *in vitro*, we transiently expressed HA RN-tre wild type, HA RN-tre M13, or empty vector in 293T cells and immunoprecipitated RN-tre using HA-antibody prior to incubation with [γ-^{32}P]GTP-loaded Rab5. Analysis of comparable amounts of immunopurified HA RN-tre, showed a reproducible decrease in [γ-^{32}P]GTP hydrolyzed in the RN-tre M13 samples compared with the RN-tre wild type samples, suggesting that loss of serine phosphorylation decreases RN-tre GAP activity *in vitro* (Fig. 7*B*). Thus, collec-

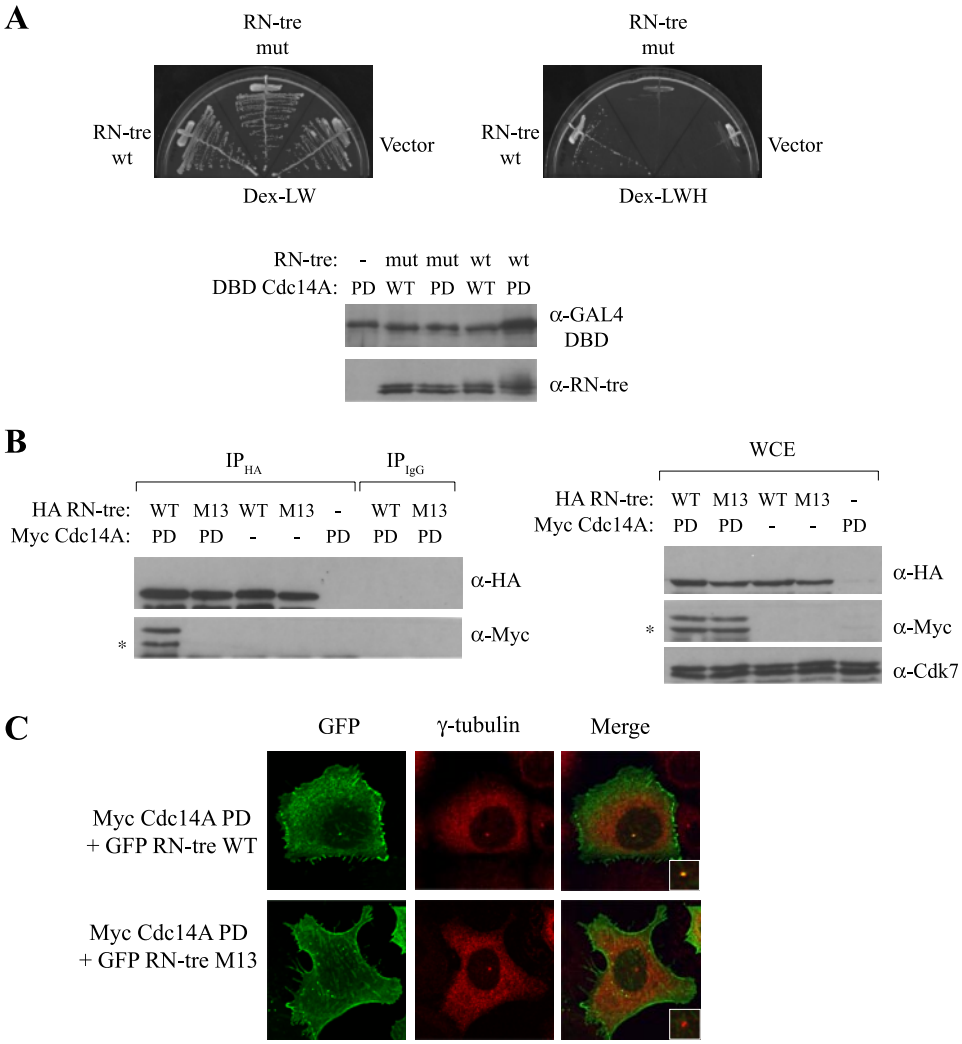

FIGURE 6. **The RN-tre phospho-deficient mutant M13 is defective in Cdc14A association but not in membrane localization.** *A*, CG1945 yeast cells expressing the Cdc14A PD bait were mated with Y187 yeast cells expressing either RN-tre-(447–828) (*RN-tre wt*), RN-tre-(447–828) carrying S576A, S585A, S595A, S642A, S655A, S659A, S680A, S784A, S791A, and S798A (*RN-tre mut*), or vector alone. Diploid cells were tested for transcription of the HIS3 reporter gene (*left*), and extracts were analyzed for expression of bait and prey proteins. Note that the RN-tre fragment is also phosphorylated in yeast cells and that the mobility shift is abolished by the S/A mutations (*bottom*). *B*, U2-OS cells were co-transfected with HA RN-tre WT or HA RN-tre M13 in combination with the indicated Myc Cdc14A expression plasmids. Cells were harvested after 21 h, lysates were used for immunoprecipitation as indicated, and the precipitated proteins were detected with rabbit polyclonal anti-HA and mouse monoclonal anti-Myc (9E10) antibodies. *C*, confocal analysis of U2-OS cells expressing GFP-RN-tre WT or GFP-RN-tre M13 together with Myc-tagged Cdc14A PD protein, stained with mouse monoclonal anti-γ-tubulin antibody (*red*). *Merged images* are also shown. Co-localization of GFP epifluorescent signal and γ-tubulin is shown in *yellow*. Co-transfection efficiencies of GFP RN-tre fusion proteins and Myc Cdc14A PD were identical (not shown). The centrosomal region is magnified in the *inset*.

tively these experiments imply that RN-tre phosphorylation may contribute to the regulation of its GAP activity *in vivo*.

DISCUSSION

To date, our understanding of the mitotic processes controlled by the Cdc14 phosphatase family in mammalian cells has been hampered by the lack of identified physiological substrates. In this report, we have described a yeast genetic system aimed at identifying targets of hCdc14A but equally applicable to the hCdc14B isoform. Using this approach, we identified RN-tre, a Rab5-GAP, as a novel binding partner of hCdc14A. Several lines of evidence suggest that RN-tre is a physiological substrate of Cdc14A. First, the Cdc14A/RN-tre interaction is highly dynamic, and a stable complex is only formed with a catalytically inactive Cdc14A (C278S) mutant (Figs. 1 and 2). Second, RN-tre is modified by phosphorylation, which can be reversed by Cdc14A activity *in vitro* as well as *in vivo* (Fig. 3, *D* and *E*). Finally, phosphorylation of RN-tre appears to be necessary for efficient binding to Cdc14A (Fig. 6), and the complex can be disrupted *in vitro* by sodium tungstate, an inhibitor of Cdc14A that binds in the catalytic pocket (Fig. 3*G*).

Previously identified Cdc14A substrates include Cdh1 (30) and Cdc25A (42), both implicated in Cdk regulation, in addition to the chromosomal passenger protein INCENP (25) involved in spindle dynamics. RN-tre expands the current repertoire of known hCdc14A substrates to include a regulator of the early endocytic pathway.

RN-tre has a well documented function in membrane trafficking, acting through Rab5, a key GTPase that controls early endosome dynamics (38) and actin cytoskeleton remodeling (39). Due to its GAP activity, RN-tre is able to inhibit Rab5-dependent functions *in vivo*, including internalization of both constitutive and ligand-dependent growth factor receptors (33). In the latter process, RN-tre interacts with Eps8, a substrate of the epidermal growth factor receptor to inhibit Rab5 and thereby epidermal growth factor receptor internalization (33). In receptor tyrosine kinase-induced actin remodeling, RN-tre also participates by forming a complex with F-actin and the F-actin bundling protein, actinin-4 (39). So far, the characterization of RN-tre has been limited to its behavior in cell signaling and membrane trafficking. In this study, we report a cell cycle-dependent phosphorylation of RN-tre, raising the possibility that this Rab-GAP has an unexpected function during the unperturbed cell cycle. Although RN-tre appears to be weakly phosphorylated in cells arrested at G_1/S and in S phase, the protein is present in a hyperphosphorylated state during mitosis (Fig. 3*A*). Notably, RN-tre phosphorylation seems to be limited to a narrow window around mitosis, since it is easily observed in isolated mitotic cells but barely detectable in a G_1/S double thymidine synchronization experiment, presumably masked by the limitations in synchrony obtained with this method (data not shown). This temporal restriction of RN-tre

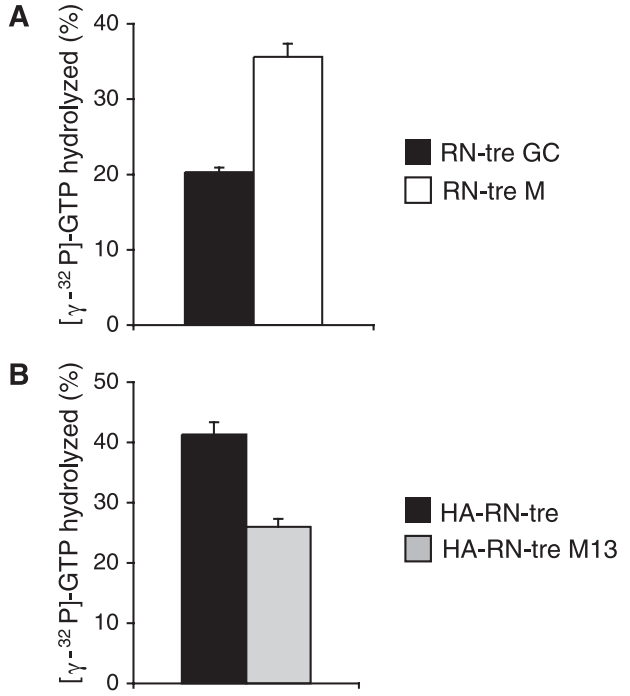

FIGURE 7. **Analysis of RN-tre activity by *in vitro* GAP assays.** *A*, endogenous RN-tre protein was immunoprecipitated from HeLa cells growing (*GC*) or synchronized at mitosis by nocodazole block (*M*) using the mouse monoclonal anti-RN-tre antibody or an irrelevant antibody as control (*CTR*). The immunoprecipitates were incubated for 5 min with [γ-^{32}P]GTP-loaded Rab5, and the decrease of radioactivity was measured with the filter-binding assay. *B*, 293T cells were transfected with HA-RN-tre WT or with HA-RN-tre M13 or with the empty vector (*CTR*). Total cellular lysates were immunoprecipitated using an anti-HA antibody. The immunoprecipitates were incubated for 3 min with [γ-^{32}P]GTP-loaded Rab5, and the decrease of radioactivity was measured with the filter-binding assay. GAP activity is expressed as the percentage of hydrolyzed [γ-^{32}P]GTP increment over background (obtained in the CTR conditions). The average background was as follows: in HeLa 31.3%, in 293T cells 17.2%. The *bar graph* is the result of three independent experiments ± S.D.

phosphorylation suggests that it may act as a switch to regulate RN-tre function. As cells exit mitosis, RN-tre phosphorylation rapidly disappears concomitant with mitotic Cdk inactivation. The kinetics of RN-tre dephosphorylation is consistent with the timing of human Cdc14A activation previously reported (24).

In agreement with the preference of hCdc14A for removing phosphorylations induced by proline-directed kinases, we found that RN-tre is an excellent substrate for Cdks *in vitro*, which was further supported by the observation that RN-tre phosphorylation status is sensitive to Cdk levels *in vivo*. For instance, overexpression of either Cdk1 or Cdk2, but not other mitotic kinases tested, resulted in increased phosphorylation of RN-tre in human cells. Also, *in vitro* kinase assays failed to show significant phosphorylation of RN-tre by the mitotic kinases Plk1 and Nek2 (data not shown). Conversely, short treatment with the Cdk inhibitor roscovitine impaired RN-tre phosphorylation (Fig. 4). This latter observation further implies that RN-tre phosphorylation is highly dynamic and balanced by opposing forces of kinase- and phosphatase activities. We believe that Cdk (and presumably Cdk1) is the prime kinase responsible for RN-tre phosphorylation during mitosis. It is clear, however, that additional kinase(s) are likely to regulate RN-tre given the complexity in the RN-tre phosphorylation pattern observed in our metabolic labeling experiments (Fig. 5). In a previous phosphoproteomic profiling study of tyrosine phosphorylation sites, it was indeed reported that RN-tre is modified on tyrosine residues Tyr^{582}, Tyr^{710}, and Tyr^{729}, consistent with its role in cell signaling (43). Curiously, we found little RN-tre phosphorylation on tyrosine residues in exponentially growing cells (Fig. 5*B*) but a significant posttranslational modification of threonine residues. The identity of the responsible kinase(s) is presently unclear.

So what aspect of RN-tre function is regulated by phosphorylation? Analysis of RN-tre subcellular distribution both at the endogenous level and after transient expression of GFP-fused RN-tre showed no detectable difference in RN-tre localization at the plasma membrane in interphase cells, compared with mitotic cells (data not shown). Furthermore, overexpression of activated Cdk kinases or hCdc14A phosphatase did not affect RN-tre localization, and the RN-tre M13 mutant defective in serine phosphorylation was still associated with membrane structures (data not shown; Fig. 6*C*). Thus, it is unlikely that phosphorylation plays a major role in RN-tre localization in human cells.

Instead, our biochemical analysis provides initial evidence that phosphorylation may modulate the catalytic activity of RN-tre (Fig. 7). Specifically, we recovered increased levels of Rab5-GAP activity in RN-tre immunoprecipitates isolated from mitotic cells compared with RN-tre derived from interphase cells. In contrast, abolishing serine phosphorylation led to a decreased GAP activity, as observed in the HA RN-tre M13 mutant. These observations, which favor the possibility that RN-tre phosphorylation positively regulates its GAP activity, should be interpreted in light of a few cautionary notes. First, the use of Rab5 in the GAP assays should be considered as a biochemical tool and not as a direct indication that phosphorylation influences the Rab5-GAP activity of RN-tre *in vivo*. Given the fact that many Rab-GAPs display promiscuity both *in vivo* and *in vitro* (44, 45), the exact physiological correlates of our biochemical findings remain to be elucidated. Second, it remains to be established whether the effects that we detected in the M13 mutant are due to lack of phosphorylation or other alterations induced by the introduced mutations. Third, and most important, our results on the M13 mutant possibly reflect an "average" computation of abrogating many phosphorylation signals in RN-tre, which are not necessarily all stimulatory. For instance, it was shown that RN-tre activity is negatively regulated by epidermal growth factor receptor (33) and that RN-tre is phosphorylated after EGF stimulation with kinetics similar to that of its GAP down-regulation. In this case, phosphorylation (which may also include Tyr modification) is apparently acting as a negative signal. Thus, the exact contribution of individual phosphorylation sites to the activity of RN-tre will require further study. Regardless, our results directly link for the first time phosphorylation of RN-tre to the modulation of its catalytic activity.

Mitosis in mammalian cells is accompanied by a general inhibition of membrane traffic, including receptor-mediated endocytosis and recycling (46), which resumes during late mitosis before completion of cytokinesis (47). The mechanisms underlying the cessation of endocytosis at the G_2/M transition are not fully elucidated but appear to involve phosphorylation events

mediated by Cdk1. For instance, phosphorylation of Rab4, a GTPase implicated in early endosome sorting, on Ser^{196} by Cdk1 during mitosis leads to its dissociation from endosomes (48). Furthermore, recombinant Cdk1-cyclin A complexes contain the ability to inhibit endocytic vesicle fusion *in vitro* (49). It is thus tempting to speculate that Cdk1-mediated RN-tre phosphorylation may contribute to mitotic cessation of endocytosis. In such a scenario, the rise in mitotic Cdk activity, as cells progress toward mitosis, induces RN-tre phosphorylation and, as a consequence, stimulates its GAP activity to lower Rab5 activity, thereby reducing endocytosis. Later, as cells exit mitosis coincident with mitotic Cdk inactivation, Cdc14A activation will trigger dephosphorylation of RN-tre and reduce its GAP activity, allowing restoration of Rab5 function. Although appealing, this hypothesis remains to be formally tested also in light of the fact that the mentioned promiscuity of Rab-GAPs poses the question of possible involvement of other Rabs. It should also be noted that the effect of mitotic phosphorylation on the GAP activity of RN-tre is not dramatic but most likely acts to fine tune the catalytic activity. In support, we found that the RN-tre M13 mutant, when overproduced, still retains the ability to severely impair endocytosis of the transferrin receptor (data not shown).

Interestingly, RN-tre contains a TBC homology domain present in the yeast proteins Bub2 and Cdc16. These proteins act as GAP proteins for the GTPases Tem1 and Spg1, which are the upstream components in the MEN and the septation initiation network signaling pathways, respectively. Intriguingly, in budding yeast, Cdc14 interacts with the Bub2/Bfa1 two-component GAP, and Cdc14-induced dephosphorylation of the complex in late anaphase is thought to modulate its GAP activity toward Tem1 (50). Our data suggest that a similar scenario involving Cdc14A and RN-tre may exist in human cells.

To date, only homologues of the downstream MEN components Cdc14 and the Dbf2-Mob1 kinase complex have been identified in humans (10). Whether RN-tre and Rab5 (or other putative Rab substrates of RN-tre) act as the functional equivalent of Bub2/Bfa1 and Tem1 in mitotic regulation is an intriguing possibility that warrants further investigation.

An important question that remains is where Cdc14A and RN-tre encounter each other in the cell. Cdc14A is predominantly located at centrosomes in interphase but is evicted from this organelle in mitosis, where it disperses into the cytosol, and a pool translocates to the mitotic spindle (24). At this point, Cdc14A could easily associate with RN-tre in the cytosol or in the vicinity of the plasma membrane to direct its dephosphorylation. In addition, ectopic Cdc14A and RN-tre can form a complex at the centrosome during interphase (Fig. 2, *B* and *C*). In fact, in an independent study, we have recently observed that a pool of endogenous RN-tre localizes to the centrosome, where it can interact with Cdc14A,[5] suggesting that RN-tre has a function at the centrosome, which may be regulated by Cdc14A.

The proline-rich C-terminal domain of RN-tre harboring the majority of phosphorylation sites has previously been shown to direct the interaction with Eps8 (51) and actinin-4 (39). Whether the cell cycle-dependent phosphorylation of RN-tre affects such protein-protein interactions or other aspects of RN-tre function remains to be determined in future studies. Further detailed analysis and mapping of individual phosphorylation sites in RN-tre is clearly needed to fully elucidate the role of phosphorylation and the function of this GAP in cell cycle progression in human cells. Nevertheless, our study has established a link between the cell cycle machinery and a protein of the endocytic pathway. Interestingly, several recent studies have demonstrated mitotic cell cycle functions for classical endocytic/trafficking proteins (52–54), suggesting the need for dialog to coordinate membrane dynamics with cell cycle events.

Finally, characterization of additional putative hCdc14A targets identified in the genetic substrate trapping system should broaden the spectrum of Cdc14A substrates and thus prove informative in elucidating, at the molecular level, the exact processes in human cells controlled by this conserved phosphatase.

Acknowledgments—We thank Drs. S. Levi, M. Brandeis, and J. Lukas for plasmids. We thank Joan Christensen for technical support. We are grateful to members of the Department of Cell Cycle and Cancer, in particular Dr. Jiri Lukas, for helpful discussions.

REFERENCES

1. Taylor, G. S., Liu, Y., Baskerville, C., and Charbonneau, H. (1997) *J. Biol. Chem.* **272,** 24054–24063
2. Li, L., Ernsting, B. R., Wishart, M. J., Lohse, D. L., and Dixon, J. E. (1997) *J. Biol. Chem.* **272,** 29403–29406
3. Bardin, A. J., and Amon, A. (2001) *Nat. Rev.* **2,** 815–826
4. Shirayama, M., Matsui, Y., and Toh, E. A. (1994) *Mol. Cell. Biol.* **14,** 7476–7482
5. Bardin, A. J., Visintin, R., and Amon, A. (2000) *Cell* **102,** 21–31
6. Pereira, G., Hofken, T., Grindlay, J., Manson, C., and Schiebel, E. (2000) *Mol. Cell* **6,** 1–10
7. Lee, S. E., Frenz, L. M., Wells, N. J., Johnson, A. L., and Johnston, L. H. (2001) *Curr. Biol.* **11,** 784–788
8. Shou, W., Seol, J. H., Shevchenko, A., Baskerville, C., Moazed, D., Chen, Z. W., Jang, J., Shevchenko, A., Charbonneau, H., and Deshaies, R. J. (1999) *Cell* **97,** 233–244
9. Visintin, R., Hwang, E. S., and Amon, A. (1999) *Nature* **398,** 818–823
10. Stegmeier, F., and Amon, A. (2004) *Annu. Rev. Genet.* **38,** 203–232
11. Azzam, R., Chen, S. L., Shou, W., Mah, A. S., Alexandru, G., Nasmyth, K., Annan, R. S., Carr, S. A., and Deshaies, R. J. (2004) *Science* **305,** 516–519
12. Jensen, S., Geymonat, M., and Johnston, L. H. (2002) *Curr. Biol.* **12,** R221–R223
13. Schwab, M., Lutum, A. S., and Seufert, W. (1997) *Cell* **90,** 683–693
14. Visintin, R., Craig, K., Hwang, E. S., Prinz, S., Tyers, M., and Amon, A. (1998) *Mol. Cell* **2,** 709–718
15. Higuchi, T., and Uhlmann, F. (2005) *Nature* **433,** 171–176
16. Pereira, G., and Schiebel, E. (2003) *Science* **302,** 2120–2124
17. McCollum, D., and Gould, K. L. (2001) *Trends Cell Biol.* **11,** 89–95
18. Cueille, N., Salimova, E., Esteban, V., Blanco, M., Moreno, S., Bueno, A., and Simanis, V. (2001) *J. Cell Sci.* **114,** 2649–2664
19. Trautmann, S., Wolfe, B. A., Jorgensen, P., Tyers, M., Gould, K. L., and McCollum, D. (2001) *Curr. Biol.* **11,** 931–940
20. Wolfe, B. A., and Gould, K. L. (2004) *EMBO J.* **23,** 919–929
21. Gruneberg, U., Glotzer, M., Gartner, A., and Nigg, E. A. (2002) *J. Cell Biol.* **158,** 901–914
22. Saito, R. M., Perreault, A., Peach, B., Satterlee, J. S., and van den Heuvel, S. (2004) *Nat. Cell Biol.* **6,** 777–783
23. Mailand, N., Lukas, C., Kaiser, B. K., Jackson, P. K., Bartek, J., and Lukas, J.

[5] V. Margaria, S. Jensen, L. Virgili, J. Bartek, F. Bussolino, P. P. Di Fiore, and L. Lanzetti, unpublished data.

(2002) *Nat. Cell Biol.* **4,** 317–322
24. Kaiser, B. K., Zimmerman, Z. A., Charbonneau, H., and Jackson, P. K. (2002) *Mol. Biol. Cell* **13,** 2289–2300
25. Gruneberg, U., Neef, R., Honda, R., Nigg, E. A., and Barr, F. A. (2004) *J. Cell Biol.* **166,** 167–172
26. Cho, H. P., Liu, Y., Gomez, M., Dunlap, J., Tyers, M., and Wang, Y. (2005) *Mol. Cell. Biol.* **25,** 4541–4551
27. Asakawa, K., and Toh-e, A. (2002) *Genetics* **162,** 1545–1556
28. Wang, W. Q., Sun, J. P., and Zhang, Z. Y. (2003) *Curr. Topics Med. Chem.* **3,** 739–748
29. Gray, C. H., Good, V. M., Tonks, N. K., and Barford, D. (2003) *EMBO J.* **22,** 3524–3535
30. Bembenek, J., and Yu, H. (2001) *J. Biol. Chem.* **276,** 48237–48242
31. Fields, S., and Sternglanz, R. (1994) *Trends Genet.* **10,** 286–292
32. Jensen, S., Geymonat, M., Johnson, A. L., Segal, M., and Johnston, L. H. (2002) *J. Cell Sci.* **115,** 4977–4991
33. Lanzetti, L., Rybin, V., Malabarba, M. G., Christoforidis, S., Scita, G., Zerial, M., and Di Fiore, P. P. (2000) *Nature* **408,** 374–377
34. Sorensen, C. S., Syljuasen, R. G., Falck, J., Schroeder, T., Ronnstrand, L., Khanna, K. K., Zhou, B. B., Bartek, J., and Lukas, J. (2003) *Cancer Cell* **3,** 247–258
35. Ridley, A. J., Self, A. J., Kasmi, F., Paterson, H. F., Hall, A., Marshall, C. J., and Ellis, C. (1993) *EMBO J.* **12,** 5151–5160
36. Zhang, Z. Y., and Wu, L. (1997) *Biochemistry* **36,** 1362–1369
37. Fukada, M., Kawachi, H., Fujikawa, A., and Noda, M. (2005) *Methods* **35,** 54–63
38. Zerial, M., and McBride, H. (2001) *Nat. Rev.* **2,** 107–117
39. Lanzetti, L., Palamidessi, A., Areces, L., Scita, G., and Di Fiore, P. P. (2004) *Nature* **429,** 309–314
40. Gallego, M., and Virshup, D. M. (2005) *Curr. Opin. Cell Biol.* **17,** 197–202
41. Traverso, E. E., Baskerville, C., Liu, Y., Shou, W., James, P., Deshaies, R. J., and Charbonneau, H. (2001) *J. Biol. Chem.* **276,** 21924–21931
42. Esteban, V., Vazquez-Novelle, M. D., Calvo, E., Bueno, A., and Sacristan, M. P. (2006) *Cell Cycle* **5,** 2894–2898
43. Brill, L. M., Salomon, A. R., Ficarro, S. B., Mukherji, M., Stettler-Gill, M., and Peters, E. C. (2004) *Anal. Chem.* **76,** 2763–2772
44. Albert, S., and Gallwitz, D. (1999) *J. Biol. Chem.* **274,** 33186–33189
45. Haas, A. K., Fuchs, E., Kopajtich, R., and Barr, F. A. (2005) *Nat. Cell Biol.* **7,** 887–893
46. Sager, P. R., Brown, P. A., and Berlin, R. D. (1984) *Cell* **39,** 275–282
47. Schweitzer, J. K., Burke, E. E., Goodson, H. V., and D'Souza-Schorey, C. (2005) *J. Biol. Chem.* **280,** 41628–41635
48. van der Sluijs, P., Hull, M., Webster, P., Male, P., Goud, B., and Mellman, I. (1992) *Cell* **70,** 729–740
49. Woodman, P. G., Adamczewski, J. P., Hunt, T., and Warren, G. (1993) *Mol. Biol. Cell* **4,** 541–553
50. Pereira, G., Manson, C., Grindlay, J., and Schiebel, E. (2002) *J. Cell Biol.* **157,** 367–379
51. Matoskova, B., Wong, W. T., Nomura, N., Robbins, K. C., and Di Fiore, P. P. (1996) *Oncogene* **12,** 2679–2688
52. Miserey-Lenkei, S., Couedel-Courteille, A., Del Nery, E., Bardin, S., Piel, M., Racine, V., Sibarita, J. B., Perez, F., Bornens, M., and Goud, B. (2006) *EMBO J.* **25,** 278–289
53. Royle, S. J., Bright, N. A., and Lagnado, L. (2005) *Nature* **434,** 1152–1157
54. Thompson, H. M., Cao, H., Chen, J., Euteneuer, U., and McNiven, M. A. (2004) *Nat. Cell Biol.* **6,** 335–342

Regulation of the Rab5 GTPase-activating Protein RN-tre by the Dual Specificity Phosphatase Cdc14A in Human Cells

Letizia Lanzetti, Valentina Margaria, Fredrik Melander, Laura Virgili, Myung-Hee Lee, Jiri Bartek and Sanne Jensen

J. Biol. Chem. 2007, 282:15258-15270.
doi: 10.1074/jbc.M700914200 originally published online March 19, 2007
